

Local Stability Analysis and Simulation of Omicron Virus Spread Using the Omicron SSvIR Model

Susila Bahri, *Member, IAENG*, Ainil Mardiyah, *Member, IAENG*, Ahmad Iqbal Baqi, *Member, IAENG*, and Abqorry Zakiyyah

Abstract— Vaccination does not guarantee that every individual is free from Omicron virus infection, so there is no guarantee that the spread of the Omicron virus will be reduced. This study aims to analyze the spread of the Omicron virus with various vaccination rates, namely 10%, 50%, and 100%, with the Next Generation Matrices method. The resulting basic reproductive number values are $\mathfrak{R}_0 = 0.8416 < 1$, $\mathfrak{R}_0 = 0.6252 < 1$, and $\mathfrak{R}_0 = 0.3217 < 1$. Based on these numbers and the eigenvalue stability theorem, the types of disease-free equilibrium points for the three vaccination rates $\xi^0 = (0.2308; 0.7692; 0; 0)$, $\xi^0 = (0.0567; 0.9434; 0; 0)$, and $\xi^0 = (0.0291; 0.9708; 0; 0)$ are locally asymptotically stable. Numerical simulation using the fourth-order Runge Kutta method was carried out using Maple software. The simulation results state that the greater the vaccination rate, the more the population is vaccinated. As a result, the number of infected individuals decreases and inhibits the spread of the Omicron virus.

Index Terms— mathematical modelling, numerical simulation, Omicron, SSvIR model, Vaccine, stability analysis, Next Generation Matrices, Fourth Order Runge Kutta

I. INTRODUCTION

OMICRON (B.1.1.529) is a new COVID-19 variant that first appeared in South Africa, and its transmission was detected faster than other COVID-19 variants [1]. According to WHO, the virus has the same symptoms as other COVID-19 types and can also cause severe illness or death [2]. Although the virus can attack individuals who have been vaccinated [3], vaccination remains essential to reduce the risk posed by the virus [4]. On November 26, 2021, an independent institution that aims to monitor the development of the COVID-19 virus, the Technical Advisory Group on Virus Evolution (TAG-VE),

The manuscript received on August 1, 2023; revised March 15, 2024.

Andalas University supported this work through the Indexed Publication Scheme for 2022.

Susila Bahri is a senior lecturer in the Mathematics and Data Science Department at the University of Andalas, Indonesia. (Corresponding author, e-mail: susilabahri@sci.unand.ac.id).

Ainil Mardiyah is an undergraduate student in the Mathematics and Data Science Department at the University of Andalas, Indonesia. (e-mail: ainilmardiyah14@gmail.com).

Ahmad Iqbal Baqi is a lecturer in the Mathematics and Data Science Department at the University of Andalas, Indonesia. (e-mail: baqi@sci.unand.ac.id).

Abqorry Zakiyyah is an undergraduate student in the Mathematics and Data Science Department at the University of Andalas, Indonesia. (e-mail: abqorryz@gmail.com).

suggested that WHO should designate the Omicron virus as a Variant of Concern (VOC) [2].

Mathematicians from different parts of the world have conducted studies on COVID-19, particularly on the Omicron variant [5]. They used Atalanga Balamu's derivative definition to come up with a fractional version of the Omicron mutation model in South Africa. This model was then transformed into a piecewise differential equation and simulated to estimate the effect of contact rate parameters on the infected compartment. Another group of researchers [6] constructed a model called $SEI_a I_q I_s R$, which is also a fractional piecewise differential equation system. They used the Partial Rank Correlation Coefficient (PRCC) method to determine the influential parameters in reducing Omicron infection in the population in southern Africa. Later on, another study [7] discussed a higher-order nonlinear mathematical model that considered vaccinated individuals and asymptomatic individuals, as well as the progress of vaccination and the decline of immunity against Omicron in the US and worldwide.

An analysis was conducted by an Indonesian mathematician [8] to determine the stability of the SEIR COVID-19 model in Indonesia. The study also involved numerical simulations, which found that the healing of COVID-19 can be accelerated with vaccines and that maximum isolation can slow the spread of COVID-19 in Indonesia. Another study [9] utilized the Weighted Markov Chain (MWMC) model to predict the occurrence of Omicron in Indonesia and calculate the average time of new daily cases. The research indicated that there is a 40% possibility of many cases with an interval of 50-100 occurring every 2.5 days and a 20% probability of the number of cases with an interval of 100-760 happening every five days. Finally, [10] conducted a study that investigated three vaccine distribution strategies: no vaccine, random distribution, and targeted distribution. The study was applied in five and eight districts in the West Java province of Indonesia. From the study, it was revealed that targeted vaccination can significantly reduce the number of infected cases, and it is necessary to increase the number of vaccines for individual protection to be more optimal.

We developed a mathematical model of SS_vIR to analyze the impact of vaccination on the spread and dynamics of Omicron cases in Indonesia, using actual Indonesian data. This model aims to examine how much vaccination can affect

the spread and dynamics of Omicron cases in Indonesia. We used this model to calculate the Basic Reproduction Number, which indicates the potential transmission of the virus from infected individuals to susceptible individuals. We conducted a stability analysis of the equilibrium point, which is the solution of the model or system of nonlinear equations, to identify disease-free and endemic conditions in the population. Additionally, we carried out simulations of several values of vaccination parameters using the model to estimate the spread of the Omicron virus that disappears or does not produce epidemics.

II. METHOD

The modelling of the Omicron epidemic, incorporating vaccination parameters, was applied to actual data from Indonesia. The basic reproduction number was calculated using the Next Generation Matrices method [11] under the assumption that the infected sub-compartment remains unchanged at the disease-free equilibrium point. Subsequently, this reproduction number was employed to establish the endemic equilibrium point. The stability of the disease-free equilibrium point was determined based on the eigenvalue theorem [12]. In contrast, the type of local stability of the endemic equilibrium point was determined through Routh's Theorem [13]. MAPLE software was used to simulate the effect of vaccination on Omicron virus transmission with various values of vaccination parameters.

III. FINDINGS AND DISCUSSION

A. Formulation of SSVIR Omicron Model

In this epidemiological context of Omicron, the human population is classified into four groups: the Susceptible without Vaccinated group, the Susceptible with Vaccinated group, the Infected group and the Recovered group. The model formulated assuming that vaccinated individuals are still susceptible to infection by the virus is presented in the schematic diagram shown in Figure 1.

The parameters used in Figure 1 $\beta, \delta, \mu, a, b, c,$ and e , respectively, represent the natural birth rate, the natural death rate, the mortality rate due to the Omicron virus, the vaccination rate of susceptible individuals without vaccination, the contact rate of susceptible individuals without vaccination with infected individuals, the contact rate of susceptible individuals with vaccination with infected individuals, and the recovery rate.

Based on Figure 1, the mathematical model of Omicron SSVIR can be expressed as a system of ordinary differential equations as follows:

$$\begin{aligned} \frac{dS}{dt} &= \beta - \delta S - aS - bSI \\ \frac{dS_v}{dt} &= aS - \delta S_v - cSI \\ \frac{dI}{dt} &= bSI + cS_v I - (\delta + \mu + e)I \\ \frac{dR}{dt} &= eI - \delta R \end{aligned} \tag{1}$$

where $N(t) = S(t) + S_v(t) + I(t) + R(t)$ and the

parameters $\beta, \delta, \mu, a, b, c, e$ are positive constants.

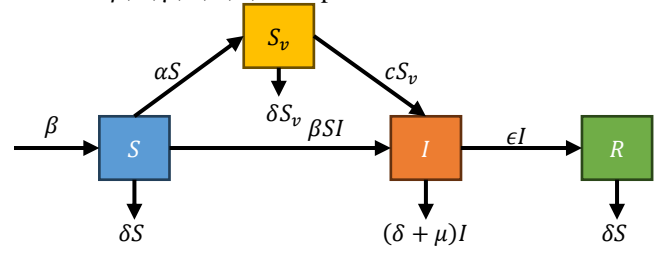


Fig. 1. SSVIR Model

The population is not constant $\frac{dN}{dt} \neq 0$ [14], which can be proven by the following:

$$\begin{aligned} \frac{dN}{dt} &= \frac{dS}{dt} + \frac{dS_v}{dt} + \frac{dI}{dt} + \frac{dR}{dt} \\ &= \beta - \mu I - \delta(S + S_v + I + R) \\ &= \beta - \mu I - \delta N. \end{aligned}$$

B. Equilibrium Point and Basic Reproduction Number (\mathfrak{R}_0)

In a mathematical model describing the spread of a disease, there exist two categories of equilibrium points: the disease-free equilibrium point (ξ^0) and the endemic equilibrium point (ξ^*). The two equilibrium points can be identified by setting each equation within the system (1) equal to zero. It will result in the following system:

$$\beta - \delta S - aS - bSI = 0 \tag{2}$$

$$aS - \delta S_v - cSI = 0 \tag{3}$$

$$bSI + cS_v I - (\delta + \mu + e)I = 0 \tag{4}$$

$$eI - \delta R = 0 \tag{5}$$

1) Disease-Free Equilibrium Point (ξ^0)

The disease-free equilibrium point (ξ^0) is a fixed point that represents a condition where there is no disease in the population $I = 0$ [15], thus obtaining the following expression:

$$\xi^0 = (S^0, S_v^0, I^0, R^0) = \left(\frac{\beta}{\delta + a}, \frac{a\beta}{\delta(\delta + a)}, 0, 0 \right). \tag{6}$$

2) Basic Reproduction Number (\mathfrak{R}_0)

Based on [12], the Jacobian matrix of the infected subsystem $\frac{dI}{dt}$ for the disease-free equilibrium point (ξ^0) is as follows:

$$J_{\xi^0} = \begin{bmatrix} \frac{b\beta}{\delta + a} + \frac{(ac\beta)}{\delta(\delta + a)} - (\delta + \mu + e) \end{bmatrix}. \tag{7}$$

The decomposition of matrix (7) yields:

$$J_{\xi^0} = \left[\frac{b\beta}{\delta + a} + \frac{(ac\beta)}{\delta(\delta + a)} \right] + [-(\delta + \mu + e)],$$

with

$$\begin{aligned} T &= \left[\frac{b\beta}{\delta + a} + \frac{(ac\beta)}{\delta(\delta + a)} \right], \\ \Sigma &= [-(\delta + \mu + e)]. \end{aligned}$$

Furthermore, using the spectral radius [8], we obtain:

$$\mathfrak{R}_0 = \rho(-T\Sigma^{-1}) \tag{8}$$

$$= \frac{\beta(b\delta + ac)}{\delta(a + \delta)(\mu + \delta + e)}$$

3) Endemic Equilibrium Point (ξ^*)

The endemic equilibrium point $\xi^* = (S^*, S_V^*, I^*, R^*)$ represents a point that indicates the occurrence of disease spread in a population where $S \neq 0, S_V \neq 0, I \neq 0, R \neq 0$ [8]. By using equations (2)-(5), the endemic equilibrium point (ξ^*) is given by:

$$\xi^* = (S^*, S_V^*, I^*, R^*) = \left(\frac{\beta}{\delta + a + bI^*}, \frac{a\beta}{(\delta + a + bI^*)(\delta + cI^*)}, I^*, \frac{eI^*}{\delta} \right), \tag{9}$$

where I^* is a positive root of

$$A_1(I)^2 + A_2I + A_3(1 - \mathfrak{R}_0) = 0 \tag{10}$$

and

$$A_1 = (\delta + \mu + e)(bc) > 0, \tag{11}$$

$$A_2 = (\delta + \mu + e)(c\delta + ac + b\delta) - bc\beta, \tag{12}$$

$$A_3 = \delta(\delta + a)(\delta + \mu + e) > 0. \tag{13}$$

Then, in order to ensure that the root of equation (10)

$$I^* = \frac{-A_2 \pm \sqrt{(A_2)^2 - 4A_1A_3(1 - \mathfrak{R}_0)}}{2A_1}, \tag{14}$$

If $\mathfrak{R}_0 > 1$, then $A_3(1 - \mathfrak{R}_0) < 0$ and equation (10) have two real roots, one positive and the other negative. When $\mathfrak{R}_0 \leq 1$, equation (10) has two real roots, both of which are negative. Then, by using $\mathfrak{R}_0 \leq 1$, the following result is obtained:

$$\begin{aligned} \mathfrak{R}_0 &\leq 1 \\ \beta(b\delta + ac) &\leq \delta(a + \delta)(\mu + \delta + e) \\ \beta &\leq \frac{\delta(a + \delta)(\mu + \delta + e)}{b\delta + ac}. \end{aligned} \tag{15}$$

Next, by substituting equation (15) into equation (12), we obtain

$$\begin{aligned} A_2 &= (\delta + \mu + e)(c\delta + ac + b\delta) - bc\beta \\ &= (\delta + \mu + e) \left(\frac{b\delta^2 + ac^2\delta + ac^2 + acb\delta}{b\delta + ac} \right) > 0, \end{aligned} \tag{16}$$

C. Stability Analysis of Equilibrium Point

In analyzing the stability of equilibrium points of the system (1), linearization is performed by using the Jacobian matrix [12].

$$J_{S,S_V,I,R} = \begin{bmatrix} -\delta - a - bl & 0 & -bS & 0 \\ a & -\delta - cl & -cS_V & 0 \\ bl & cl & bS + cS_V - (\mu + \delta + e) & 0 \\ 0 & 0 & e & -\delta \end{bmatrix}. \tag{17}$$

The type of stability for the two equilibrium points is obtained through the following analysis.

1) Disease-Free Equilibrium Point

Based on the value of the basic reproduction number \mathfrak{R}_0 , the stability of the disease-free equilibrium point is determined by the following Theorem 1.

Theorem 1:

The disease-free equilibrium point ξ_0 for equation (6) of the system (1) is asymptotically stable if $\mathfrak{R}_0 < 1$. Otherwise, this equilibrium point is considered unstable [8], [15].

Proof.

Based on equation (17), the Jacobian matrix at the disease-free equilibrium point ξ_0 is given by

$$J_{S,S_V,I,R} = \begin{bmatrix} -\delta - a & 0 & -bS^0 & 0 \\ a & -\delta & -cS_V^0 & 0 \\ 0 & 0 & bS^0 + cS_V^0 - (\mu + \delta + e) & 0 \\ 0 & 0 & e & -\delta \end{bmatrix}. \tag{18}$$

Then, the characteristic equation of the matrix J_{ξ^0} using the identity matrix I is given by:

$$\begin{aligned} \det(J_{\xi^0} - \lambda I) &= 0 \\ \det \begin{pmatrix} -\delta - a - \lambda & 0 & -bS^0 & 0 \\ a & -\delta - \lambda & -cS_V^0 & 0 \\ 0 & 0 & bS^0 + cS_V^0 - (\mu + \delta + e) - \lambda & 0 \\ 0 & 0 & e & -\delta - \lambda \end{pmatrix} &= 0 \end{aligned} \tag{19}$$

Therefore, the eigenvalues of the Jacobian matrix J_{ξ^0} are obtained as follows:

$$\lambda_1 = -\delta < 0, \tag{20}$$

$$\lambda_2 = -\delta - a < 0, \tag{21}$$

$$\lambda_3 = -\delta < 0, \tag{22}$$

$$\lambda_4 = (\mu + \delta + e)(\mathfrak{R}_0 - 1). \tag{23}$$

The Stability Theorem of Eigenvalues plays an important role in understanding the stability of the disease-free equilibrium point ξ^0 . According to the theorem, the local asymptotic stability of this point is determined by the condition that $\lambda_j < 0$ for $j = 1, 2, 3, \dots, n$ [12]. When we look at the equations (20)-(22), we can see that the eigenvalues $\lambda_1, \lambda_2, \lambda_3$ are all less than 0. To satisfy the stability criteria, we need λ_4 to be less than 0 as well. The stability of the disease-free equilibrium point ξ^0 depends on the value of \mathfrak{R}_0 . If \mathfrak{R}_0 is less than 1, then all eigenvalues of the Jacobian matrix J_{ξ^0} will exhibit negative real parts, resulting in the local asymptotic stability of the disease-free equilibrium point ξ^0 . However, if \mathfrak{R}_0 is greater than 1, certain eigenvalues of the Jacobian matrix J_{ξ^0} will have positive real parts, leading to the instability of the disease-free equilibrium point ξ^0 .

2) Endemic Equilibrium Point

Based on the value of basic reproduction number \mathfrak{R}_0 , the stability of the endemic equilibrium point is determined according to the following Theorem 2.

Theorem 2:

If $\mathfrak{R}_0 > 1$, then the endemic equilibrium point ξ^* for equation (9) of the system (1) is asymptotically stable. Otherwise, this equilibrium point is considered unstable [8].

Proof.

Based on equation (17), the Jacobian matrix at the endemic equilibrium point ξ^* [16] is given by:

$$J_{S,S_V,I,R} = \begin{bmatrix} -\delta - a - bI^* & 0 & -bS^* & 0 \\ a & -\delta - cI^* & -cS_V^* & 0 \\ bI^* & cI^* & bS^* + cS_V^* - (\mu + \delta + e) & 0 \\ 0 & 0 & e & -\delta \end{bmatrix}$$

$$= \begin{bmatrix} -\frac{\beta}{S^*} & 0 & -bS^* & 0 \\ a & \frac{aS^*}{S_V^*} & -cS_V^* & 0 \\ bI^* & cI^* & 0 & 0 \\ 0 & 0 & e & -\delta \end{bmatrix} \tag{24}$$

where

$$-(\delta + a + bI^*) = -\frac{\beta}{S^*}, \tag{25}$$

$$-(\delta + cI^*) = -\frac{aS^*}{S_V^*}, \tag{26}$$

$$bS^* + cS_V^* - (\mu + \delta + e) = 0. \tag{27}$$

Next, the characteristic equation of the matrix J_{ξ^*} using the identity matrix I is as follows:

$$\det(J_{\xi^*} - \lambda I) = 0$$

$$\det \begin{pmatrix} -\frac{\beta}{S^*} - \lambda & 0 & -bS^* & 0 \\ a & -\frac{aS^*}{S_V^*} - \lambda & -cS_V^* & 0 \\ bI^* & cI^* & -\lambda & 0 \\ 0 & 0 & e & -\delta - \lambda \end{pmatrix} = 0$$

$$(\delta + \lambda) \left[\lambda^3 + \left(\frac{\beta}{S^*} + \frac{aS^*}{S_V^*} \right) \lambda^2 + \left(\frac{\beta}{S^*} \frac{aS^*}{S_V^*} + b^2 S^* I^* + c^2 S_V^* I^* \right) \lambda + I^* \left(abc S^* + \frac{aS^*}{S_V^*} b^2 S^* + \frac{\beta}{S^*} c^2 S_V^* \right) \right] = 0 \tag{28}$$

$$\lambda^3 + C_1 \lambda^2 + C_2 \lambda + I^* C_3 = 0,$$

with

$$C_1 = \frac{\beta}{S^*} + \frac{aS^*}{S_V^*}, \tag{29}$$

$$C_2 = \frac{a\beta}{S_V^*} + b^2 S^* I^* + c^2 S_V^* I^*, \tag{30}$$

$$C_3 = (abc S^* + \frac{aS^*}{S_V^*} b^2 S^* + \frac{\beta}{S^*} c^2 S_V^*). \tag{31}$$

To determine whether all the roots of the polynomial equation (28) have negative real parts or not, the Routh criteria, as revealed by Routh's Theorem [13], are utilized, resulting in the Routh array as follows,

λ^3	1	C_2
λ^2	C_1	$I^* C_3$
λ^1	r	0
λ^0	s	0

Where

$$r = C_1 C_2 - \frac{I^* C_3}{C_1}$$

$$= \frac{\frac{a\beta^2}{S^* S_V^*} + (\delta + bI^*) b^2 S^* I^* + \frac{a^2 \beta S^*}{(S_V^*)^2} + aS^* I^* ((b - c)^2 + bc)}{C_1}, \tag{32}$$

$$s = \frac{r I^* C_3}{r}$$

$$= I^* \left(abc S^* + \frac{aS^*}{S_V^*} b^2 S^* + \frac{\beta}{S^*} c^2 S_V^* \right). \tag{33}$$

Both r and s must be positive to ensure that the roots of the polynomial equation (28) are negative. Additionally, if

the endemic equilibrium point I^* is positive, then r and s should also be greater than 0. It is important because if the value of \mathfrak{R}_0 is greater than 1, which indicates an endemic equilibrium point ξ^* , then it is considered to be locally asymptotically stable. On the other hand, if either r or s is negative, then the roots of equation (28) will have positive real parts, which will lead to a negative value of I^* . As a result, if R_0 is less than 1, indicating an endemic equilibrium point ξ^* , it is considered to be unstable.

D. The solution of the SS_VIR model using the fourth-order Runge-Kutta method

The system of equations (1) can be rewritten as follows,

$$\frac{dS}{dt} = f_1(t, S, S_V, I, R) = \beta - \delta S(t) - a S(t) - b S(t) I(t),$$

$$\frac{dS_V}{dt} = f_2(t, S, S_V, I, R) = a S(t) - \delta S_V(t) - c S_V(t) I(t)$$

$$\frac{dI}{dt} = f_3(t, S, S_V, I, R) = b S(t) I(t) + c S_V(t) I(t) - (\delta + \mu + e) I(t),$$

$$\frac{dR}{dt} = f_4(t, S, S_V, I, R) = e I(t) - \delta R(t)$$
(34)

Based on [17], the system of equations (34) can be transformed into fourth-order Runge-Kutta equations as follows,

$$S_{n+1} = S_n + \frac{h}{6} (k_{1S} + 2k_{2S} + 2k_{3S} + k_{4S}), \tag{35}$$

$$(S_V)_{n+1} = (S_V)_n + \frac{h}{6} (k_{1S_V} + 2k_{2S_V} + 2k_{3S_V} + k_{4S_V}), \tag{36}$$

$$I_{n+1} = I_n + \frac{h}{6} (k_{1I} + 2k_{2I} + 2k_{3I} + k_{4I}), \tag{37}$$

$$R_{n+1} = R_n + \frac{h}{6} (k_{1R} + 2k_{2R} + 2k_{3R} + k_{4R}), \tag{38}$$

with

$$k_{1S} = f_1(t_n, S_n, (S_V)_n, I_n, R_n),$$

$$k_{1S_V} = f_2(t_n, S_n, (S_V)_n, I_n, R_n),$$

$$k_{1I} = f_3(t_n, S_n, (S_V)_n, I_n, R_n),$$

$$k_{1R} = f_4(t_n, S_n, (S_V)_n, I_n, R_n),$$

$$k_{2S} = f_1 \left(t_n + \frac{1}{2}h, S_n + \frac{1}{2}k_{1S}h, (S_V)_n + \frac{1}{2}k_{1S_V}h, I_n + \frac{1}{2}k_{1I}h, R_n + \frac{1}{2}k_{1R}h \right),$$

$$k_{2S_V} = f_2 \left(t_n + \frac{1}{2}h, S_n + \frac{1}{2}k_{1S}h, (S_V)_n + \frac{1}{2}k_{1S_V}h, I_n + \frac{1}{2}k_{1I}h, R_n + \frac{1}{2}k_{1R}h \right),$$

$$k_{2I} = f_3 \left(t_n + \frac{1}{2}h, S_n + \frac{1}{2}k_{1S}h, (S_V)_n + \frac{1}{2}k_{1S_V}h, I_n + \frac{1}{2}k_{1I}h, R_n + \frac{1}{2}k_{1R}h \right),$$

$$k_{2R} = f_4 \left(t_n + \frac{1}{2}h, S_n + \frac{1}{2}k_{1S}h, (S_V)_n + \frac{1}{2}k_{1S_V}h, I_n + \frac{1}{2}k_{1I}h, R_n + \frac{1}{2}k_{1R}h \right),$$

$$k_{3S} = f_1 \left(t_n + \frac{1}{2}h, S_n + \frac{1}{2}k_{2S}h, (S_V)_n + \frac{1}{2}k_{2S_V}h, I_n + \frac{1}{2}k_{2I}h, R_n + \frac{1}{2}k_{2R}h \right),$$

$$k_{3S_V} = f_2 \left(t_n + \frac{1}{2}h, S_n + \frac{1}{2}k_{2S}h, (S_V)_n + \frac{1}{2}k_{2S_V}h, I_n + \frac{1}{2}k_{2I}h, R_n + \frac{1}{2}k_{2R}h \right),$$

$$k_{3I} = f_3 \left(t_n + \frac{1}{2}h, S_n + \frac{1}{2}k_{2S}h, (S_V)_n + \frac{1}{2}k_{2S_V}h, I_n + \frac{1}{2}k_{2I}h, R_n + \frac{1}{2}k_{2R}h \right),$$

$$k_{3R} = f_4 \left(t_n + \frac{1}{2}h, S_n + \frac{1}{2}k_{2S}h, (S_V)_n + \frac{1}{2}k_{2S_V}h, I_n + \frac{1}{2}k_{2I}h, R_n + \frac{1}{2}k_{2R}h \right),$$

$$k_{4S} = f_1(t_n + h, S_n + k_{3S}h, (S_V)_n + k_{3S_V}h, I_n + k_{3I}h, R_n + k_{3R}h),$$

$$k_{4S_V} = f_2(t_n + h, S_n + k_{3S}h, (S_V)_n + k_{3S_V}h, I_n + k_{3I}h, R_n + k_{3R}h),$$

$$k_{4I} = f_3(t_n + h, S_n + k_{3S}h, (S_V)_n + k_{3S_V}h, I_n + k_{3I}h, R_n + k_{3R}h),$$

$$k_{4R} = f_4(t_n + h, S_n + k_{3S}h, (S_V)_n + k_{3S_V}h, I_n + k_{3I}h, R_n + k_{3R}h),$$

t_n represents time, and h represents the step size.

E. The solution of the SS_VIR model using the fourth-order Runge-Kutta method

The model is simulated using MAPLE software, utilizing the initial variable values provided in Table I and the corresponding parameter values outlined in Table II.

TABLE I
VARIABLE VALUES

Variable	Estimated Value	Source
N	1	[18]
$S(0)$	0.8401	[19]
$S_V(0)$	0.1599	[19],[20]
$I(0)$	0.00004	[21],[22]
$R(0)$	0.00002	Estimated

TABLE II
PARAMETER VALUES

Parameter	Estimated Value	Source
β	0.03/day	Estimated
δ	0.03/day	Estimated
μ	0.0007/day	Estimated
$a(1)$	10%/day	Assumed
$a(2)$	50%/day	Assumed
$a(3)$	100%/day	Assumed
b	0.3/day	Estimated
$c(1)$	0.6/day	Estimated
$c(2)$	0.4/day	Estimated
$c(3)$	0.2/day	Estimated
e	0.6/day	Estimated

By substituting the parameter values from Table II into the system (1), the equilibrium points and the basic reproduction number of the SS_VIR model are determined as follows:

$$\begin{aligned}
 \frac{dS}{dt} &= 0.03 - 0.03 S(t) - a S(t) - 0.3 S(t) I(t), \\
 \frac{dS_V}{dt} &= a S(t) - 0.03 S_V(t) - c S(t) I(t) \\
 \frac{dI}{dt} &= 0.3 S(t) I(t) + c S_V(t) I(t) - (0.03 \\
 &\quad + 0.0007 + 0.6) I(t), \\
 \frac{dR}{dt} &= 0.6 I(t) - 0.03 R(t)
 \end{aligned}
 \tag{39}$$

The parameter values can be substituted with several simulation values, $a(1)$, $a(2)$, and $a(3)$, along with the initial values $S(0)$, $S_V(0)$, $I(0)$, and $R(0)$ in Table I. Then, using equation (7), the basic reproduction number is obtained and presented in Table III.

TABLE III
SIMULATION RESULTS OF \mathfrak{R}_0

Simulation	Vaccination Parameter	Contact rate of S_V with I	\mathfrak{R}_0
1	$a(1) = 10\%$	$c(1) = 0.6$	$\mathfrak{R}_0 = 0.8416 < 1$
2	$a(2) = 50\%$	$c(2) = 0.4$	$\mathfrak{R}_0 = 0.6252 < 1$
3	$a(3) = 100\%$	$c(3) = 0.2$	$\mathfrak{R}_0 = 0.3217 < 1$

After conducting three simulations, it was determined that the basic reproduction number (\mathfrak{R}_0) for each simulation was less than 1. As a result, it can be inferred that the disease-free equilibrium point ξ^0 is asymptotically stable [1]. Using the parameter values listed in Table II to solve equations (6)

and (20) – (23), Table IV displays the equilibrium values for the disease-free state, as well as the eigenvalues associated with each simulation.

A numerical simulation has been performed using the fourth-order Runge-Kutta method to investigate how vaccination affects population dynamics during the spread of the Omicron virus. The simulation used the initial values described in Table I and the parameters specified in Table II, with the parameter a being assigned with various values. From Table III, it can be interpreted that an increase in the number of people vaccinated (a) affects the ability of the virus to infect. In other words, the contact rate between sub-individuals who have been vaccinated with infected sub-individuals c decreases. This condition means that the number of sub-individuals infected also decreases so that the spread of the virus is hampered. At the same time, the number of recovered sub-individuals increased. The results of the simulation for the Omicron virus transmission model are presented visually in Figures 2, 3, 4, and 5.

The administration of 10% of vaccines exclusively to the susceptible subpopulation without prior vaccination, as depicted in Figure 2, exhibits an extended duration required to diminish the size of this subpopulation. Concurrently, this reduction leads to an escalation in the count of vaccinated susceptible subpopulations, reaching approximately 214,744,174 individuals, as illustrated in Figure 3. The allocation of 50% of vaccines to the susceptible subpopulation without vaccination results in a relatively swift decrease in the number of susceptible subpopulations without vaccination, as portrayed in Figure 2. However, this approach also corresponds to an increase in the number of vaccinated susceptible subpopulations, reaching approximately 263,333,883 individuals in Figure 3. Lastly, the administration of 100% of vaccines to the susceptible subpopulation without prior vaccination induces a rapid surge in the number of vaccinated susceptible subpopulations, reaching approximately 270,873,666 individuals, as indicated in Figure 3. In Figure 4, by administering 10% vaccine, the disease-free equilibrium point can be reached in approximately 60 days. Then, by administering 50% and 100% vaccines, respectively, the equilibrium point can be reached within 36 and 22 days. In Figure 5, for administering 10% vaccine, the maximum number of recovered subpopulation individuals was 25,691 on day 11. In comparison, with 50% vaccine administration, the maximum number of 23,178 recovered subpopulation individuals was attained in approximately nine days. Moreover, the complete distribution of vaccines resulted in the highest recovery number of individuals in the subpopulation, reaching 16,755 within around six days.

The results of this study highlight the effectiveness of administering the vaccine in reducing individuals infected with Omicron. It emphasizes the crucial role of COVID-19 vaccination in controlling the rapid spread of the Omicron variant. These simulation findings are essential in enhancing strategies aimed at managing and controlling the number of COVID-19 cases in Indonesia, with a particular focus on reducing the impact of the Omicron variant.

IV. CONCLUSION

Comprehensive results were obtained after an extensive

research study analyzing the SS_VIR model under various vaccination conditions, indicating that Indonesia is not experiencing an epidemic caused by the Omicron virus. Moreover, the present vaccination initiative has been

successfully achieved in impeding the transmission of the virus. Consequently, it is essential to prioritize individual vaccination as a proactive approach to avoid and mitigate the risk of exposure to the virus.

TABLE IV
VALUES OF DISEASE-FREE EQUILIBRIUM AND EIGENVALUES FOR EACH SIMULATION

Simulation	S^0	S_V^0	I^0	R^0	λ_1	λ_2	λ_3	λ_4	\mathfrak{R}_0
1	0.2307	0.7692	0	0	-0.03	-0.13	-0.03	-0.0999	$\mathfrak{R}_0 = 0.8416 < 1$
2	0.0566	0.9434	0	0	-0.03	-0.53	-0.03	-0.2364	$\mathfrak{R}_0 = 0.6252 < 1$
3	0.0291	0.9708	0	0	-0.03	-1.03	-0.03	-0.4278	$\mathfrak{R}_0 = 0.3217 < 1$

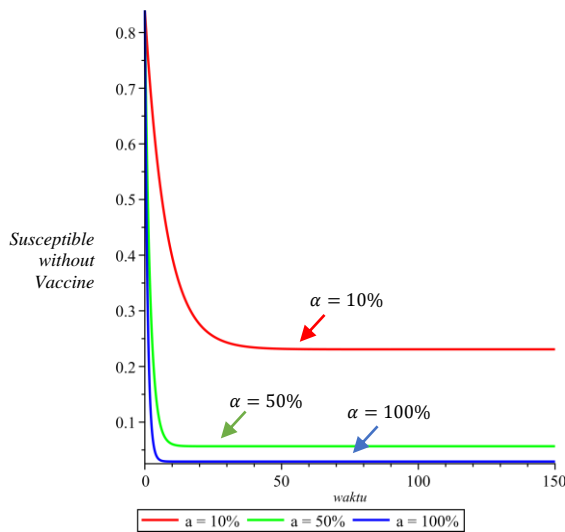


Fig. 2. Variation in the number of Susceptible without Vaccine (S) populations for different values of a

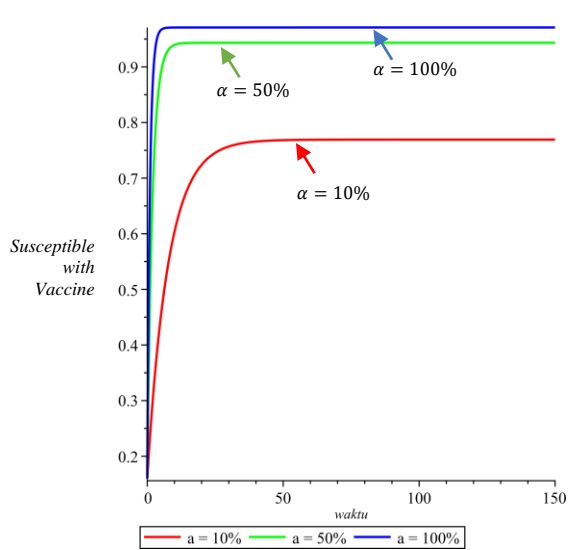


Fig. 3. Variation in the number of Susceptible with Vaccine (S_V) population for different values of a

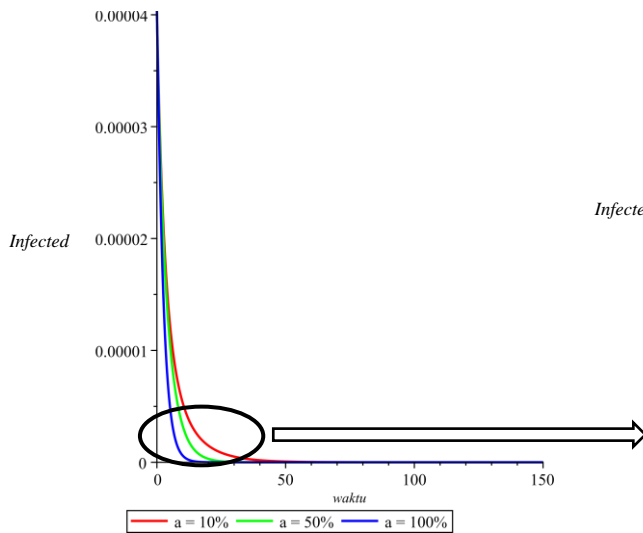
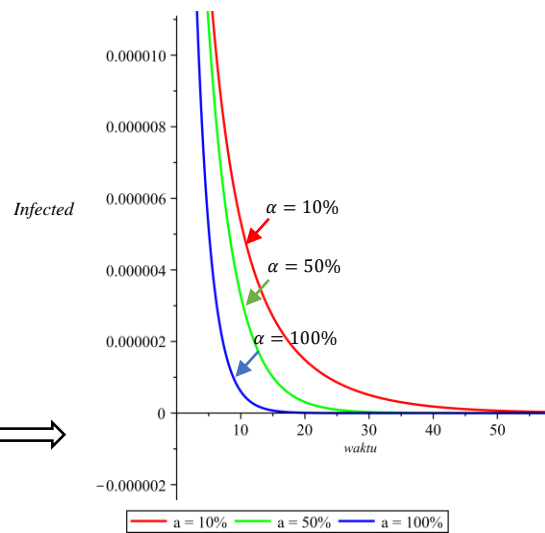


Fig. 4. Variation in the number of Infected (I) population for different values of a



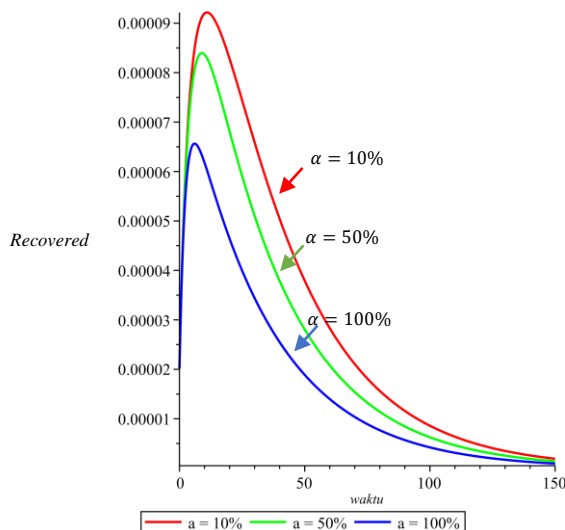


Fig. 5. Variation in the number of Recovered (R) population for different values of α

REFERENCES

[1] World Health Organization (WHO), Classification of Omicron (B.1.1.529): SARS-CoV-2 Variant of Concern, 2022. Available: <https://www.who.int>

[2] World Health Organization (WHO), Update on Omicron, 2022. Available: <https://www.who.int>

[3] Kompas.com, Why Can Vaccinated People Still Get Infected with Omicron? Here is the Reason, 2022. Available: <https://www.kompas.com>

[4] Kompas.com, Kenapa Orang yang Sudah Vaksin Bisa Kena Omicron? Ini Alasannya, 2022. Tersedia pada: <https://www.kompas.com>

[5] Kompas.com, Vaccination Reduces the Worst Risks of Omicron, 2022. Available: [Vaksinasi Kurangi Risiko Terburuk Omicron - Infografik Katadata.co.id](https://www.kompas.com)

[6] Kompas.com, Vaksinasi Kurangi Risiko Terburuk Omicron, 2022. Tersedia pada: [Vaksinasi Kurangi Risiko Terburuk Omicron - Infografik Katadata.co.id](https://www.kompas.com)

[7] Khan, Muhammad Althaf, A. Abdon, "Assessing the potential impact of COVID-19 Omicron variant: Insight through a fractional piecewise model", Results in Physics, vol. 38, pp105652, 2022.

[8] Khan, Muhammad Althaf, A. Abdon, "Mathematical Modeling and Analysis of COVID-19: A Study of New Variant Omicron", Physica A, vol. 599, pp127452, 2022.

[9] González-Parra, G.; Arenas, A. J. Mathematical Modeling of SARS-CoV-2 Omicron Wave under Vaccination Effects. Computation 2023, 11, 36.

[10] Annas, Suardi., Muh. Isbar Pratama, Muh. Rifandi, Wahidah Sanusi, Syafruddin Side, "Stability Analysis and Numerical Simulation of SEIR Model for Pandemic COVID-19 Spread in Indonesia", Chaos, Solitons and Fractals, vol. 139, pp110072, 2020.

[11] Kafi, Al Rahmat., Sihombing, Anggia Abygail, "Predicting Omicron Daily New Cases in Indonesia and Its Mean Recurrence Time Using Modified Weighted Markov Chain", Journal of Research and Applications in Mathematics, vol. 6, no. 1, 2021.

[12] Fuady, Ahmad., et al., "Targeted Vaccine Allocation Could Increase the COVID-19 Vaccine Benefits Amidst Its Lack of Availability: A Mathematical Modeling Study in Indonesia", Vaccines, vol. 9, no. 5, pp462-472, 2021.

[13] Diekmann, Odo, J. A. P. Heesterbeek, and Michael G. Roberts, "The Construction of Next-Generation Matrices for Compartmental Epidemic Models", Journal of the Royal Society Interface, vol 7, no 47, pp873-885, 2010.

[14] Kelley, W. G. (2010). *The theory of differential equations (Online)*. Springer. Available: [The Theory of Differential Equations: Classical and Qualitative | SpringerLink](https://www.springer.com)

[15] Brannan, J. R., & Boyce, W. E. (2015). *Differential equations: An introduction to modern methods and applications (Online)*. John Wiley & Sons. Available: [Differential Equations: An Introduction to Modern Methods and Applications - James R. Brannan, William E. Boyce - Google Books](https://www.google.com/books)

[16] Bastin, G., "Mathematical Modeling of Biological Systems", presented at 2018 Lecture on Mathematical Modeling of Biological Systems, GBIO.

[15] Bahri, S., Fitrialitya, I., Nasution, H., Lestari, R., Fajria, L., "Analysis of the Effects of Foreign Travelers and Immigrants on Omicron Transmission in Indonesia", International Journal of Mathematics and Computer Science, vol. 19, no. 3, pp893-902, 2024.

[16] G. Suganya, and R. Senthamarai, "Impact of Awareness on the Dynamics of Pest Control in Coconut Trees - A Mathematical Model," Engineering Letters, vol. 30, no.4, pp1199-1209, 2022.

[17] Anna Silvia Purnomo, Isnani Darti, Agus Suryanto, and Wuryansari Muharini Kusumawinahyu, "Fear Effect on a Modified Leslie-Gower Predator-Prey Model with Disease Transmission in Prey Population," Engineering Letters, vol. 31, no.2, pp764-773, 2023.

[18] Side, S., Utami, A M., Sukarna., Pratama, M I., "Numerical solution of SIR model for transmission of tuberculosis by Runge-Kutta method", Journal of Physics: Conference Series, vol. 1040, no. 012021, 2018.

[19] Worldometer, Indonesia Population, 2022. Available: <https://www.worldometers.info>

[20] Covid.go.id, COVID-19 Vaccination Data (Updated as of January 1, 2022), 2022. Available: <https://covid19.go.id>

[21] Covid.go.id, Data Vaksinasi COVID-19 (Update per 1 Januari 2022), 2022. Tersedia pada: <https://covid19.go.id>

[22] Covid.go.id, COVID-19 Situation in Indonesia (Updated as of June 1, 2022), 2022. Available: <https://covid19.go.id>

[23] Covid.go.id, Situasi COVID-19 di Indonesia (Update per 1 Juni 2022), 2022. Tersedia pada: <https://covid19.go.id>

[22] Databoks, Omicron Update: Total Cases in Indonesia Reach 11,447 (Wednesday, June 1, 2022), 2022. Available: <https://databoks.katadata.co.id>

[22] Databoks, Update Omicron: Total di Indonesia Ada 11.447 Kasus (Rabu, 01 Juni 2022), 2022. Tersedia pada: <https://databoks.katadata.co.id>

[23] Detiknews, 2 Omicron Patients in Indonesia Have Died; here is the Data on the Surge in Cases in January, 2022. Available: <https://news.detik.com>

[23] Detiknews, 2 Pasien Omicron RI Meninggal, Ini Data Lonjakan Kasus di Januari, 2022. Tersedia pada: <https://news.detik.com>